



HAL
open science

Impact of historical climate change on the Southern Ocean carbon cycle

Richard J. Matear, Andrew Lenton

► **To cite this version:**

Richard J. Matear, Andrew Lenton. Impact of historical climate change on the Southern Ocean carbon cycle. *Journal of Climate*, 2008, 21, pp.5820-5834. 10.1175/2008JCLI2194.1 . hal-00770574

HAL Id: hal-00770574

<https://hal.science/hal-00770574>

Submitted on 11 Jun 2021

HAL is a multi-disciplinary open access archive for the deposit and dissemination of scientific research documents, whether they are published or not. The documents may come from teaching and research institutions in France or abroad, or from public or private research centers.

L'archive ouverte pluridisciplinaire **HAL**, est destinée au dépôt et à la diffusion de documents scientifiques de niveau recherche, publiés ou non, émanant des établissements d'enseignement et de recherche français ou étrangers, des laboratoires publics ou privés.

Impact of Historical Climate Change on the Southern Ocean Carbon Cycle

R. J. MATEAR

CSIRO Marine and Atmospheric Research, and ACE CRC, Hobart, Tasmania, Australia

A. LENTON

Laboratoire d'Océanographie et du Climat: Expérimentations et Approches Numériques (LOCEAN/IPSL), Université Pierre et Marie Curie, Paris, France

(Manuscript received 16 August 2007, in final form 1 May 2008)

ABSTRACT

Climate change over the last several decades is suggested to cause a decrease in the magnitude of the uptake of CO₂ by the Southern Ocean (Le Quere et al.). In this study, the atmospheric fields from NCEP R1 for the years 1948–2003 are used to drive an ocean biogeochemical model to probe how changes in the heat and freshwater fluxes and in the winds affect the Southern Ocean's uptake of carbon. Over this period, the model simulations herein show that the increases in heat and freshwater fluxes drive a net increase in Southern Ocean uptake (south of 40°S) while the increases in wind stresses drive a net decrease in uptake. The total Southern Ocean response is nearly identical with the simulation without climate change because the heat and freshwater flux response is approximately both equal and opposite to the wind stress response. It is also shown that any change in the Southern Ocean anthropogenic carbon uptake is always opposed by a much larger change in the natural carbon air–sea exchange. For the 1948–2003 period, the changes in the natural carbon cycle dominate the Southern Ocean carbon uptake response to climate change. However, it is shown with a simple box model that when atmospheric CO₂ levels exceed the partial pressure of carbon dioxide (pCO₂) of the upwelled Circumpolar Deep Water ($\approx 450 \mu\text{atm}$) the Southern Ocean uptake response will be dominated by the changes in anthropogenic carbon uptake. Therefore, the suggestion that the Southern Ocean carbon uptake is a positive feedback to global warming is only a transient response that will change to a negative feedback in the near future if the present climate trend continues.

Associated with the increased outgassing of carbon from the natural carbon cycle was a reduction in the aragonite saturation state of the high-latitude Southern Ocean (south of 60°S). In the simulation with just wind stress changes, the reduction in the high-latitude Southern Ocean aragonite saturation state (≈ 0.2) was comparable to the magnitude of the decline in the aragonite saturation state over the last 4 decades because of rising atmospheric CO₂ levels (≈ 0.2). The simulation showed that climate change could significantly impact aragonite saturation state in the Southern Ocean.

1. Introduction

The Southern Ocean (SO, oceans south of 40°S) has the highest annual-averaged winds over the oceans. These strong westerly winds help drive the Antarctic Circumpolar Current (ACC) eastward around Antarctica. These winds through Ekman transport also produce a northward flow, creating a divergent driven deep upwelling south of the ACC. In this region, the upwelling of middepth (2–2.5 km) water to the surface

provides a unique connection between the deep ocean and the atmosphere. This deep-ocean connection makes the Southern Ocean extremely important in controlling the storage of carbon in the ocean and in setting atmospheric CO₂ levels.

Atmospheric reanalysis products suggest that there has been a poleward movement and intensification of winds over the Southern Ocean since the 1970s (Thompson and Solomon 2002), which has been linked to a decline in SO carbon uptake over the last 3 decades (Le Quere et al. 2007). The observed wind changes are consistent with most of the Fourth Assessment Report (AR4) climate models, which simulate a poleward shift of the westerlies in the twentieth century but underes-

Corresponding author address: R. J. Matear, GPO Box 1538, Hobart 7001, Australia.
E-mail: richard.matear@csiro.au

timate the magnitude of the observed change (Yin 2005). The AR4 climate models also have a tendency to project further poleward movement and intensification of westerlies under future global warming simulations (Russell et al. 2006b; Cai and Cowan 2007; Fyfe and Saenko 2006; Miller et al. 2006). Given the importance of the SO for the air–sea exchange of carbon and the uptake of anthropogenic CO₂, a key issue is how these circulation changes will impact the air–sea exchange of carbon.

Previous studies have shown that the Southern Ocean uptake of carbon is impacted by climate change through the combined effects of ocean CO₂ solubility changes, anthropogenic uptake changes, and natural carbon cycle changes (Bopp et al. 2001; Matear and Hirst 1999; Sarmiento et al. 1998). As demonstrated by Matear and Hirst (1999), each of these terms can be of comparable magnitude. A recent study by Russell et al. (2006a) concluded that a change in the strength of the westerly winds over the SO would increase upwelling in the SO and lead to increased carbon storage in the ocean. It is important to emphasize that their conclusions on the change in the ocean storage of carbon were based only on how the anthropogenic carbon uptake changes. The analysis of Russell et al. (2006b) is missing a very important response—the natural carbon cycling response to climate change, which does impact the ocean carbon content and the air–sea carbon fluxes. Here, we explore how the changes in the strength and latitude of the westerly winds and in the heat and freshwater fluxes impact the exchange of carbon between the atmosphere and the SO. In the next section, we describe our ocean model and the model experiments. The following section presents the key results of the simulations. The final section discusses how the simulations can be used to assess both the past and future carbon uptake response of the SO to climate change. One key result of our modeling work is that for past climate change any atmospheric forcing field associated with an increase in anthropogenic CO₂ uptake is associated with a much greater outgassing of carbon resulting from changes in the natural carbon cycle.

2. Model description and experiments

We used a prognostic global 3D biogeochemical ocean general circulation model (BOGCM) to investigate changes in air–sea CO₂ fluxes under changing atmospheric forcing. The ocean general circulation module (OGCM) was based on the Z-coordinate Modular Ocean Model (MOM), version 3 (Pacanowski and Griffies 1999). The model grid has a horizontal resolution of 0.94°N–0.94°S and 1.9°E–1.9°W at the equator, with a

tapering of longitude as a function of cosine (T63–2), and 31 nonregular vertical levels, with 15 levels in the upper 500 m. To represent the effects of eddies not simulated in the model, the eddy parameterization of Gent and McWilliams (1990) was implemented. Upper-ocean mixing was parameterized by using the Chen et al. (1994) mixed layer scheme. The biogeochemical module of the BOGCM predicted dissolved inorganic carbon (DIC), alkalinity, oxygen, and phosphate fields, and is based on Lenton et al. (2006) and Matear and Hirst (2003). This same model configuration was used to investigate the interannual variability in the air–sea flux of CO₂ associated with the Southern Annular Mode (SAM; Lenton and Matear 2007) and the partial pressure of carbon dioxide (pCO₂) ocean sampling strategy for estimating Southern Ocean CO₂ uptake (Lenton et al. 2006). In general, the model reproduces the observed phosphate, oxygen, and carbon seasonality in the Southern Ocean. However, for a more detailed comparison of the model simulations with observations refer to Lenton et al. (2006) and Lenton and Matear (2007).

The model was initialized in 1850 with the values of preindustrial DIC and alkalinity from the Global Ocean Data Analysis Project (GLODAP; Sabine et al. 2005), and temperature, salinity, oxygen, and phosphate fields from the *World Ocean Atlas 2001* (WOA 2001; see Conkright et al. 2002). The model simulations used in this study followed the protocols set out in the Northern Ocean Carbon Exchange Study (NOCES)–International Carbon Cycle Model Intercomparison Project Phase 3 (OCMIP3), designed to simulate interannual variability in ocean biogeochemical models (Aumont et al. 2004). In the simulation we included two DIC tracers. The first DIC tracer, total DIC, was influenced by the observed atmospheric pCO₂ concentration from the 1850 to 2002 period (Enting et al. 1994). The second DIC tracer, preindustrial DIC, only sees an atmospheric pCO₂ concentration of 280 μatm. For these two DIC tracers, the air–sea gas exchange of CO₂ was calculated following the relationship of Wanninkhof (1992), using daily wind speed from National Centers for Environmental Prediction–National Center for Atmospheric Research (NCEP–NCAR) Global Reanalysis 1 (NCEP-1). To account for the impact of sea ice, the net CO₂ flux was scaled by the fraction of observed sea ice cover, interpolated from the global monthly climatological fields of Walsh (1978) and Zwally et al. (1983). In this study, we define a positive CO₂ flux as a flux into the ocean.

The model was forced between the years 1850 and 1948 with daily NCEP-1 wind stresses, heat, and freshwater fluxes of the year 1948 (Kalnay 1996) with both

TABLE 1. The daily forcing fields used to drive the model from 1948 to 2002 for the various experiments. Variable forcing refers to the use of forcing fields from 1948 to 2002, while 1948 denotes the use of forcing fields from only 1948. For cases where the winds are allowed to vary (total and tau), the interannually varying wind speeds are used in the calculation of the gas exchange coefficient for the air–sea CO₂ fluxes; otherwise the 1948 winds are used.

Experiment	Forcing		
	Heat flux	Freshwater flux	Winds
Total	Variable	Variable	Variable
1948	1948	1948	1948
Hflx	Variable	1948	1948
Fflx	1948	Variable	1948
Tau	1948	1948	Variable

sea surface temperature and salinity restored with a 30-day time scale to observed sea surface temperature (SST) from 1948 (Reynolds and Smith 1994) and annual sea surface salinity (SSS) climatology (Conkright et al. 2002). From the years 1945–47, the mean seasonal freshwater fluxes associated with the surface salinity relaxation were computed and applied to the subsequent years of the simulation (1948–2002). For the years 1948–2002, no additional salinity restoring was used in contrast to the Lenton and Matear (2007), which included a weak restoring to SSS climatology (2-yr restoring time scale). For the 1948–2002 period, SST was restored to the observed daily SST values (Reynolds and Smith 1994) with a 30-day time scale. We refer to the experiment where all forcing fields are varying as our “total” experiment (Table 1). Using the heat and freshwater fluxes and wind stresses from the “total” experiment, we performed additional runs where either the freshwater fluxes, heat fluxes, or wind stresses were individually allowed to vary from the 1948 values. In addition, we performed a control run where 1948 forcing fields of the total run were applied to years 1949–2002.

Ocean forcing fields

Because the forcing fields play a crucial role in the response of the oceanic uptake of carbon we will first review how the NCEP-1 forcing fields change in the SO over the 1948–2002 period. Shown in Fig. 1 are the SO-averaged forcing fields of the total experiment, which we refer to as historical climate change. Over this period all three forcing fields display a systematic trend. Both the heat and freshwater fluxes into the ocean increase while the zonal and meridional wind stresses over the ocean also increase. Note that the freshwater fluxes are the sum of the seasonal mean climatology flux calculated by relaxing the SSS values to the clima-

tology SSS field during the spinup of the model plus the NCEP-1 freshwater fluxes. The heat fluxes are the combination of a restoring flux associated with the restoration of the SST to observations and the NCEP-1 net heat flux (Fig. 1). If we plot just the heat fluxes of the NCEP-1 forcing field the trend is even greater (Fig. 2). With the relaxation term, the trend in the heat flux into the ocean is reduced because the observed SST displays no obvious trend; hence, the relaxation flux tries to reduce the heat flux going into the ocean (Fig. 2).

The NCEP-1 wind stresses display a clear trend over the 1948–2002 period (Fig. 1). The trend in the zonal wind stresses reflects both an intensification of the zonally averaged westerly maximum and a poleward movement in the zonally averaged westerly wind stress maximum (Fig. 3). This wind response is the dominant component of a more positive SAM over this period and it is attributed primarily to changes in stratospheric ozone and greenhouse gases (Arblaster and Meehl 2006). Although a more positive SAM is associated with wind changes in the SO, as discussed by Hall and Visbeck (2002) there are also clear trends to increased heat and freshwater fluxes into the SO with a more positive SAM.

NCEP-1 fields from the 1948 to 2003 period over the SO display a systematic increased and poleward shift in the westerly winds that are similar to global warming projections (Russell et al. 2006b). Although there is some question as to the validity of these changes (Marshall 2003), we use them as a proxy to explore how the oceanic uptake of carbon may change under the projected strengthening of SAM displayed in many of the AR4 climate model simulations of global warming (Yin 2005; Cai and Cowan 2007; Fyfe and Saenko 2006; Miller et al. 2006).

3. Results

The model experiments were set up to explore how both the anthropogenic and the total carbon uptake in the SO changes under varying heat fluxes, freshwater fluxes, and winds.

Over the 1948–2002 period, the model experiments displayed significant differences in their annual SO carbon uptake (Fig. 4). For total carbon uptake, the uptake for year 1948 was about 0.45 Gt C yr⁻¹ (all experiments). By 2003, the uptake had increased to 0.95 Gt C yr⁻¹ for the 1948 experiment. The experiments that when either heat or freshwater fluxes only varied the uptake by 2003 and were 1.0 and 1.3 Gt C yr⁻¹, respectively. In comparison, when only the winds changed (tau experiment) the uptake by 2003 was 0.4 Gt C yr⁻¹ a small decrease from the uptake in 1948. For the com-

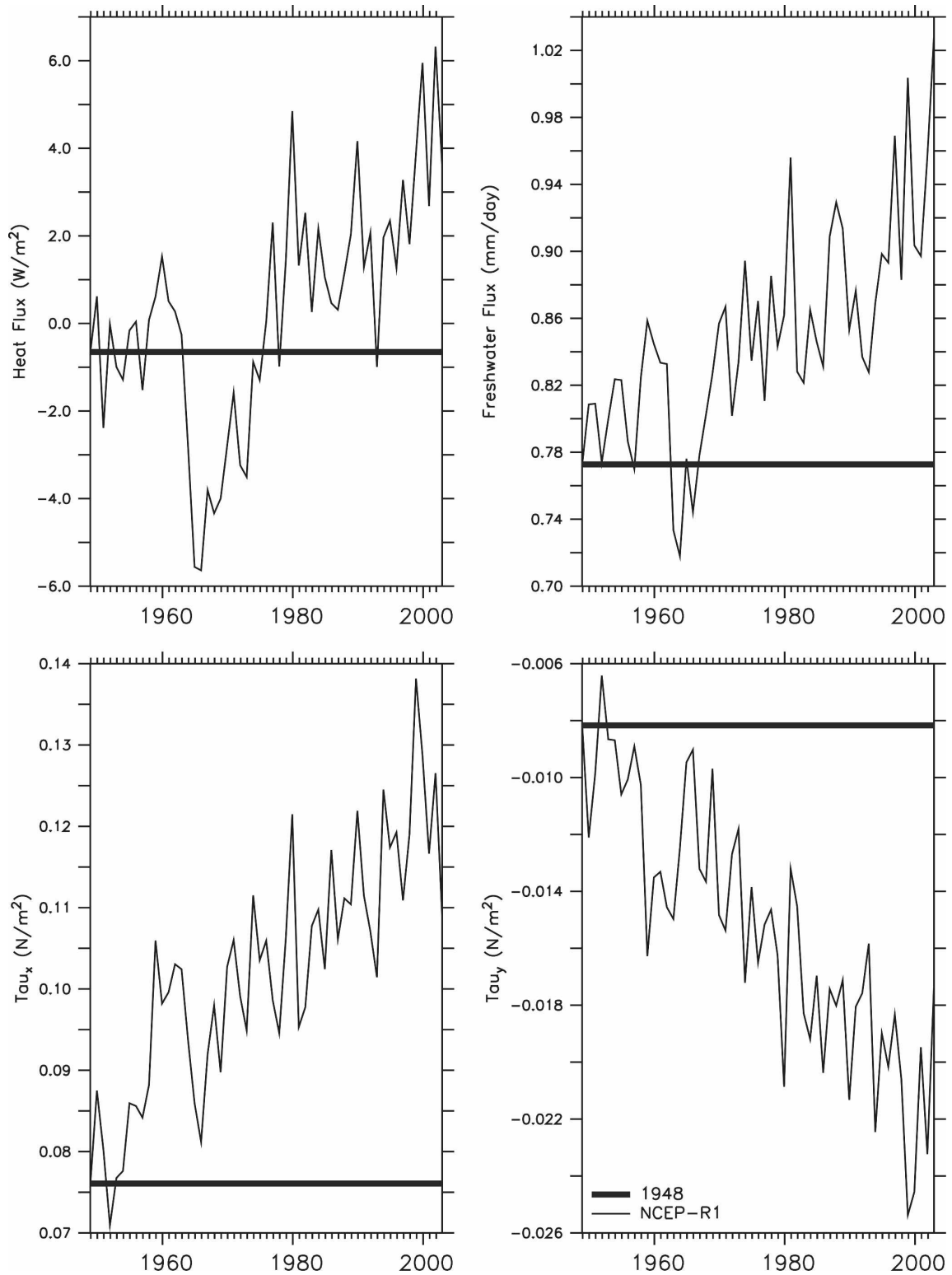


FIG. 1. SO annually averaged heat flux ($W m^{-2}$), freshwater flux ($mm day^{-1}$), longitudinal wind stress (dynes), and latitudinal wind stress (dynes) into the ocean. The experiments shown are the total experiment (thin line) and the 1948 experiment (bold line). For the wind stresses, the thin line is just the NCEP-1 fields while for the heat and freshwater fluxes the thin line is the NCEP-1 fields plus a restoring term.

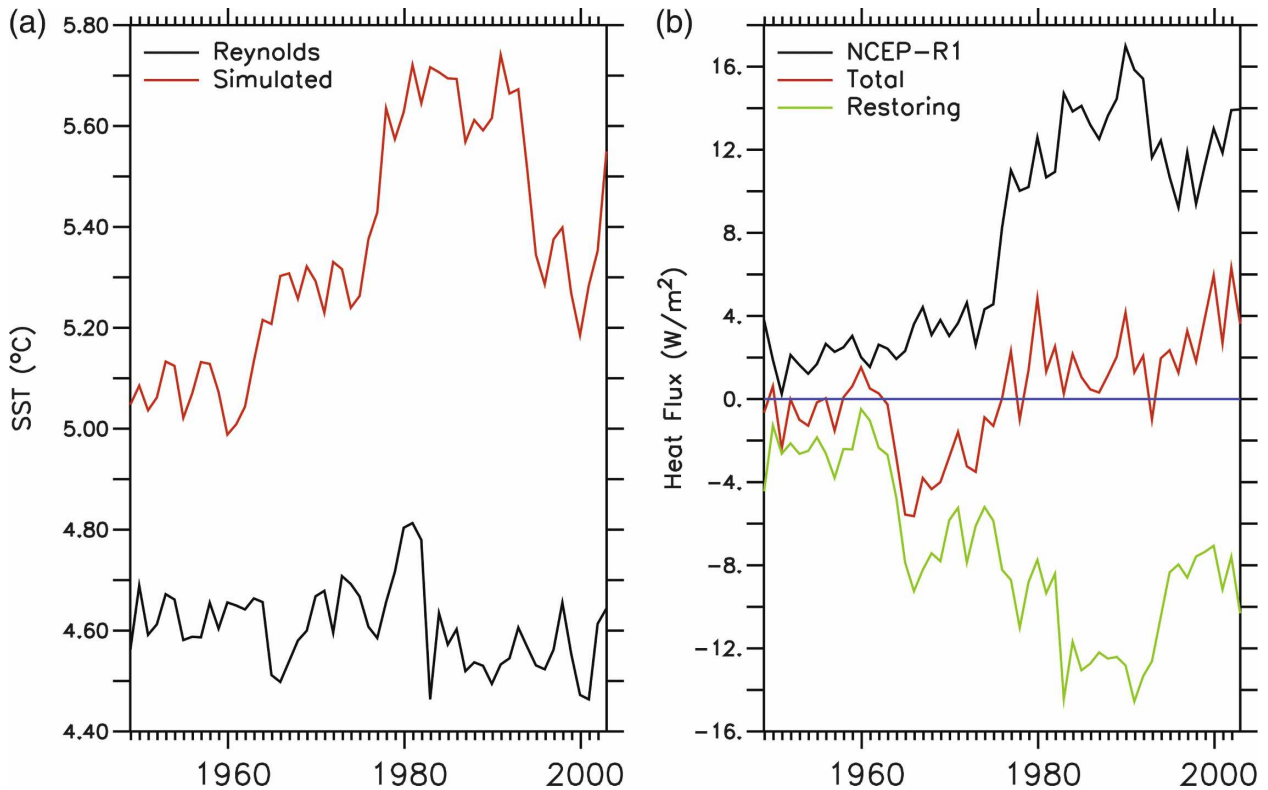


FIG. 2. SO annually averaged (a) sea surface temperature ($^{\circ}\text{C}$) observed (black line; Reynolds and Smith 1994) and simulated by the total experiment (red line); (b) net heat flux into the ocean (W m^{-2}) from the NCEP-1 fields (black line), from the total experiment (red line) and just the restoring heat flux term from the total experiment (green line), which is the red line – the black line.

bin response of heat flux, freshwater flux, and wind stress variability (total experiment) the oceanic uptake in 2003 was $0.95 \text{ Gt C yr}^{-1}$, which was similar to the value from the 1948 experiment. The consistency between the total and the 1948 experiments at the end of the simulation was not representative of the whole period. In general, the total experiment had less uptake than the 1948 experiment (Fig. 4a).

To elucidate how changes in the forcing fields impact the SO carbon uptake we show the annual mean uptake of the preindustrial carbon tracer and anthropogenic carbon (Figs. 4b,c). The anthropogenic carbon uptake was calculated as the difference between the total uptake and the uptake of the preindustrial carbon tracer. As expected for all experiments the anthropogenic carbon uptake increased from 1948 to 2003 as CO_2 levels in the atmosphere increased. The uptake in year 2003 varied between 0.65 and 1.1 Gt C yr^{-1} . The greatest uptake occurred with just wind forcing variability while the smallest uptake occurred with just freshwater flux variability. Consistent with Russell et al. (2006a), the stronger the winds were, the greater the anthropogenic carbon uptake. The uptake of the preindustrial carbon tracer showed that the natural carbon cycle responded

to climate change. The freshwater flux experiment had the greatest increase in the natural carbon uptake while the wind stress experiment had the greatest decrease in the natural carbon uptake. The model simulations demonstrated the changes in the natural carbon uptake, which are neglected in the Russell et al. (2006a) study, did influence the SO carbon uptake. As shown by the correlation coefficient between changes in anthropogenic carbon uptake and changes in natural carbon uptake, for all simulations the change in the natural carbon uptake were always opposite to the change in the anthropogenic carbon uptake (Table 2).

4. Discussion

The atmospheric changes did alter the total ocean uptake of carbon. The variability in the SO uptake of carbon reflected the variability in natural carbon cycling and the uptake of anthropogenic carbon. The atmospheric forcing fields that increased anthropogenic carbon uptake were also associated with the outgassing of carbon by the ocean from the natural carbon cycle. The strong anticorrelation between changes in the anthropogenic uptake versus the changes in the natural

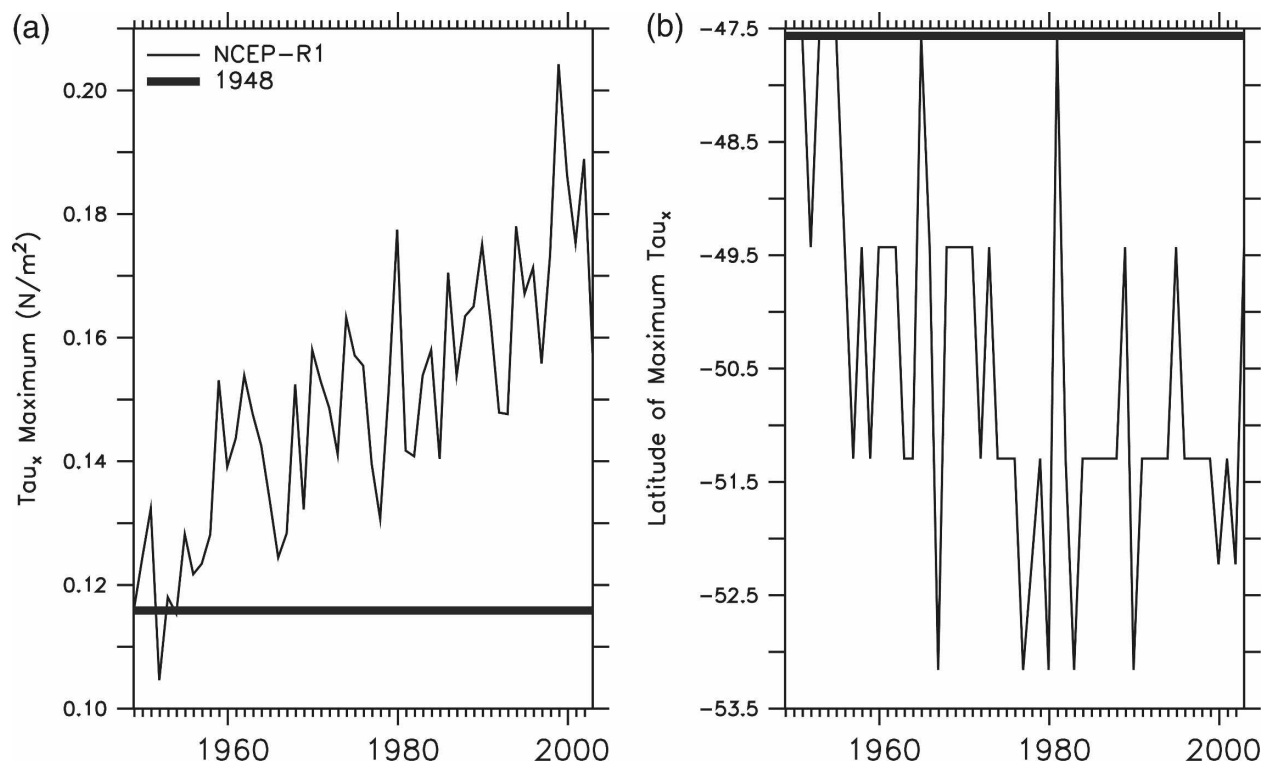


FIG. 3. In the SO: (a) the maximum zonally averaged westerly wind stress and (b) the latitude of the zonally averaged westerly wind stress maximum. The experiments shown are the total experiment (thin line) and the 1948 experiment (bold line).

carbon uptake relative to the 1948 experiment was evident in all forcing experiments (Table 2). The anticorrelation was strongest in the individual forcing experiments, but it was still significant when all forcing variability was included. The reduced correlation of the total experiment reflected the nonlinear nature of the carbon chemistry in the ocean and the SO response to atmospheric forcing, which allowed the sum of the three individual forcing experiments to deviate from the total experiment response. The regression value for the change in anthropogenic uptake versus the change in natural carbon uptake showed that for all forcing experiments the anthropogenic response was opposite and 10%–26% of the magnitude of natural carbon cycle response. Hence, over the 1948–2003 period, the total change in SO carbon uptake with climate change was dominated by changes in the natural carbon cycle.

From the total experiment, our simulations suggested little change in the ocean uptake of carbon from the 1948 experiment. Our results disagree with the recent study of Le Quere et al. (2007), which suggested that the SO uptake had declined over the last three decades because of changes in atmospheric forcing, but they were consistent with the results of Lovenduski et al. (2007, 2008). Given the competing effects of heat, fresh-

water, and wind variability on the SO carbon exchanges, how heat and freshwater fluxes are applied to the BOGCM may change the character of the SO response to climate change. In addition, when the uncertainty in the heat and freshwater fluxes were considered along with the uncertainty in the air–sea fluxes estimate of the atmospheric inversions one cannot conclude that a decline in the SO carbon uptake has occurred (Law et al. 2008). It would be useful with different ocean models to investigate the SO carbon uptake response to the different atmospheric forcing terms and assess the robustness of our simulated relationship between changes in anthropogenic and natural carbon uptake (Table 2).

In discussing how the SO carbon uptake will change under global warming it is important to consider both the anthropogenic and natural carbon cycle responses. The projected global warming increase in the uptake of anthropogenic carbon presented by Russell et al. (2006a) will be countered by an outgassing carbon from the ocean resulting from changes in the natural carbon cycling.

a. Ocean ventilation impact

We hypothesize that the link between changes in atmospheric forcing and carbon uptake was primarily through how the atmospheric forcing fields alter SO

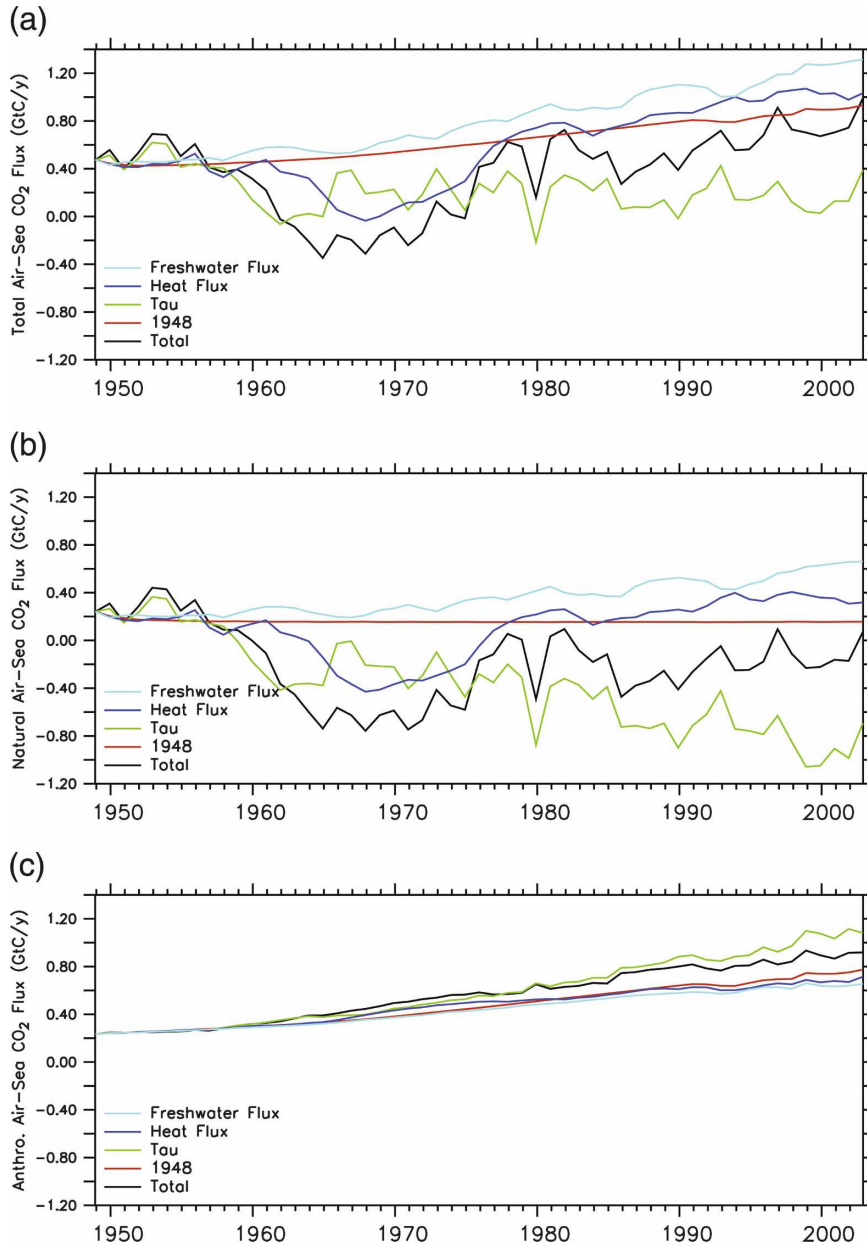


FIG. 4. Annually averaged SO uptake of (a) total carbon, (b) natural carbon, and (c) anthropogenic carbon. The different experiments use the following color coding: total experiment (black line), 1948 (red line), tau (green line), Hflx (blue line), and Fflx (cyan line).

ventilation and subduction of mode and intermediate waters. The ventilation of the ocean (exposure to the atmosphere) depends on two opposing forces: the strength of the wind-driven divergence and the strength of the stratification resulting from warming and freshening. We used the surface outcrop area of water denser than $27.1 (\sigma)$ to quantify the ventilation of the Southern Ocean (Fig. 5). This definition defines the region where the Antarctic Intermediate Water (AAIW),

or denser water, is exposed to the atmosphere. Our simulated outcrop area was comparable to the 3.1×10^6 km² area estimated from climatological data (Conkright et al. 2002). From our experiments, the wind stress variability increased the outcropping area by about 40% while freshwater flux variability reduced the area by nearly the same amount (Fig. 5b).

For all forcing experiments, interannual variability in the SO natural carbon flux was strongly negatively cor-

TABLE 2. The correlation coefficient of the annual mean SO carbon fluxes with annual mean outcrop area of water denser than 27.1 σ_θ (ocean ventilation proxy). Also given is the correlation coefficient and regression value of the changes in the annual mean SO anthropogenic carbon uptake vs the change in the annual mean SO natural carbon fluxes. The changes in the carbon fluxes are determined by subtracting the fluxes from the 1948 experiment. The regression value gives the change in the anthropogenic carbon fluxes per unit change in the natural carbon fluxes.

Experiment	Correlation with ocean ventilation		Changes in SO anthropogenic carbon fluxes versus natural carbon fluxes	
	Natural	Anthropogenic	Correlation	Regression
Total	-0.8165	0.1050	-0.52	-0.10
1948	—	—		
Hflx	-0.8888	0.8507	-0.81	-0.12
Fflx	-0.9612	0.9542	-0.96	-0.22
Tau	-0.9617	0.9045	-0.91	-0.26

related with ocean ventilation (Table 2). This reflected the fact that DIC concentrations in the SO increased with depth (e.g., Sabine et al. 2005) and the increased ocean ventilation increased the supply of DIC-elevated deep water to the surface ocean, increasing the outgassing of CO₂ from the ocean. The strong correlation for all of the forcing experiments supported our hypothesis that variability in ocean ventilation controlled SO carbon uptake variability. Further, ocean ventilation variability may provide a means of quantifying SO carbon uptake variability. For such an approach, it would be interesting to investigate the relationship between ventilation changes and SO carbon uptake with different ocean models.

For the wind stress, heat flux, and freshwater flux experiments the interannual variability in the SO anthropogenic carbon uptake relative to 1948 experiment were also strongly positively correlated with variability in ocean ventilation (Table 2). However, the total experiment, which includes variability in all three forcing terms, showed a much poorer correlation with ocean ventilation variability. The following two reasons may explain the poor correlation: First, the opposing response of changes in the winds to changes in freshwater and heat fluxes produced much less variability in the total experiment's carbon uptake compared to either the wind or the freshwater experiment; hence, the magnitude of the response was small and it may be more difficult to detect. Second, the ocean ventilation diagnostic may be a poor proxy for the key process that drives anthropogenic carbon uptake variability: the subduction of mode and intermediate waters (McNeil et al. 2003). The ability to use this diagnostic proxy held for the individual forcing experiments but failed for the total experiment. In an attempt to define a better proxy for variability in the subduction of mode and intermediate water we correlated the variability in the cross-sectional area at 30°S of water with a σ_θ between 26.8 and 27.2 with variability in anthropogenic carbon up-

take. This gave a much higher correlation (0.6) supporting the hypothesis that changes in the subduction of mode and intermediate waters was a key process in driving the variability in the uptake of anthropogenic carbon in the total experiment. The simulations showed that the subduction changes were more influenced by the wind changes than by either the heat or the freshwater flux changes.

b. Export production variability

The simulated changes in SO carbon uptake were dominated by the physical response of the ocean to variability in atmospheric forcing. In the simulation, changes in export production were small (Fig. 6) and the increased nitrate supply associated with increased DIC supply did not stimulate enough new production to overcome the elevated carbon in the surface water. The simulated increases in export production only occurred on the northern boundary of the high-nutrient low-chlorophyll (HNLC) area of the SO where the increased upwelling of nutrients did relieve the nutrient limitation and enhance export production (Fig. 6b). This occurred in the simulation because export production did not depend on iron, and because south of 50°S the surface ocean was not macronutrient limited; injecting more macronutrients into the upper ocean did not stimulate increased export production.

Our simulated biological response can be justified in three ways. First, in most of the SO phytoplankton are not nitrate limited and at present the subducted AAIW and SAMW do contain nonzero nitrate concentrations (Trull et al. 2001). Therefore, supplying more nitrate to the surface water was not expected to stimulate more production. The observed high nitrate concentrations in the SO surface water and the iron fertilization experiments suggest that iron (Fe) limitation is the cause of the high nitrate concentrations. Second, the upwelling of more Fe-rich deep water would not alleviate the iron limitation and increase biological

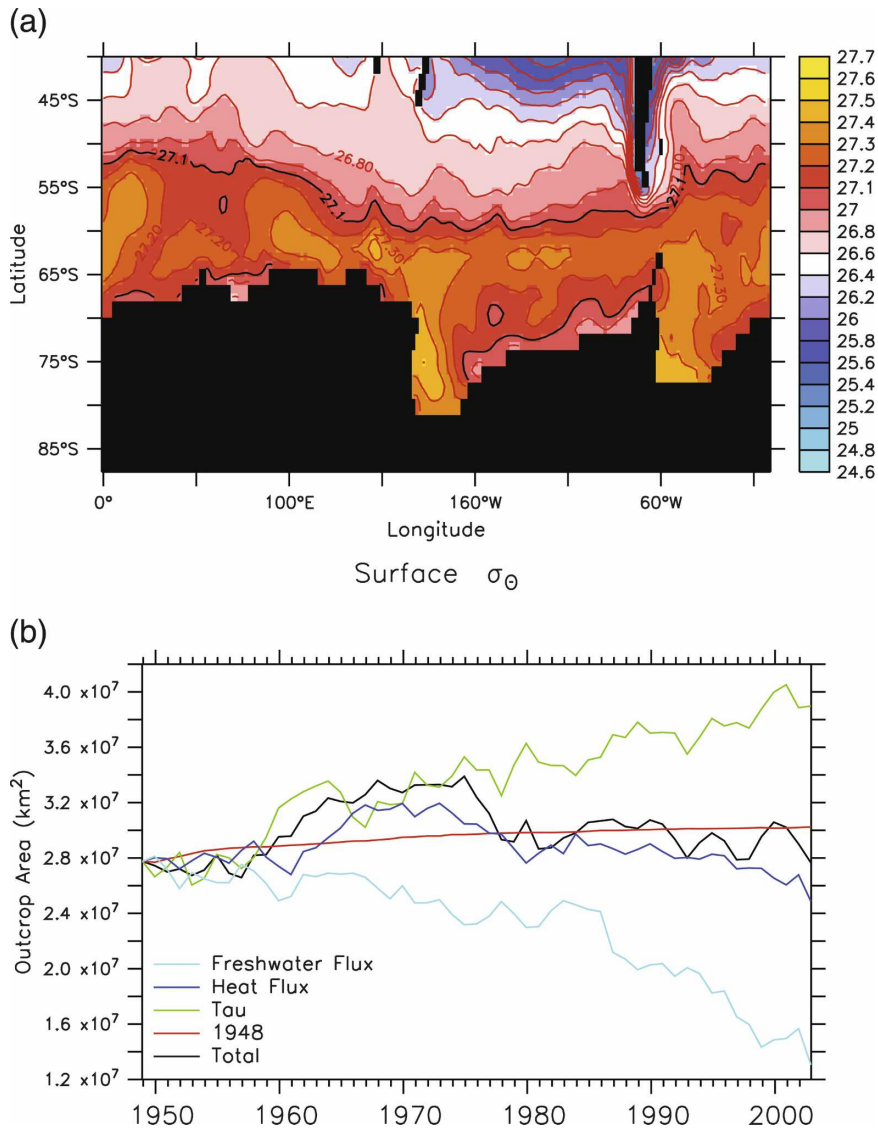


FIG. 5. (a) Annually averaged sea surface density for the year 1948. The black line denotes 27.1 contour line. (b) Outcrop area in the SO (km^2) of water with a density greater than 27.1. The color coding of the experiments follows Fig. 4.

utilization of macronutrients because the nitrate–iron ratio of the upwelled water still has excess nitrate relative to Fe (A. Bowie 2008, personal communication). Therefore, even if extra Fe is brought into the system it will not be sufficient to draw down the additional nitrate and carbon supply. Third, although upwelling of deep water would supply more Fe to increase export production, the additional export of carbon from the upper ocean would be small given the observed range in SO deep-water Fe concentrations of 0.4–2.8 nM (Löscher et al. 1997) and the observed carbon–iron (C:Fe) ratio of organic matter (Buesseler et al. 2004). Hence, these three conditions all supported a weak link

between atmospheric forcing and export production and our small simulated interannual variability in export production. As in our model, we expect in the SO that export production is decoupled from the nutrient supply.

The increased nutrient supply translates to increased nutrients in the subducted SAMW and AAIW. The increased nutrient concentration in the subducted mode and intermediate water will eventually elevate export production outside the SO (Sarmiento et al. 2004), but this will be delayed until these water masses return to the upper ocean in the equatorial region (Rodgers et al. 2003). Hence, the ocean carbon cycle is

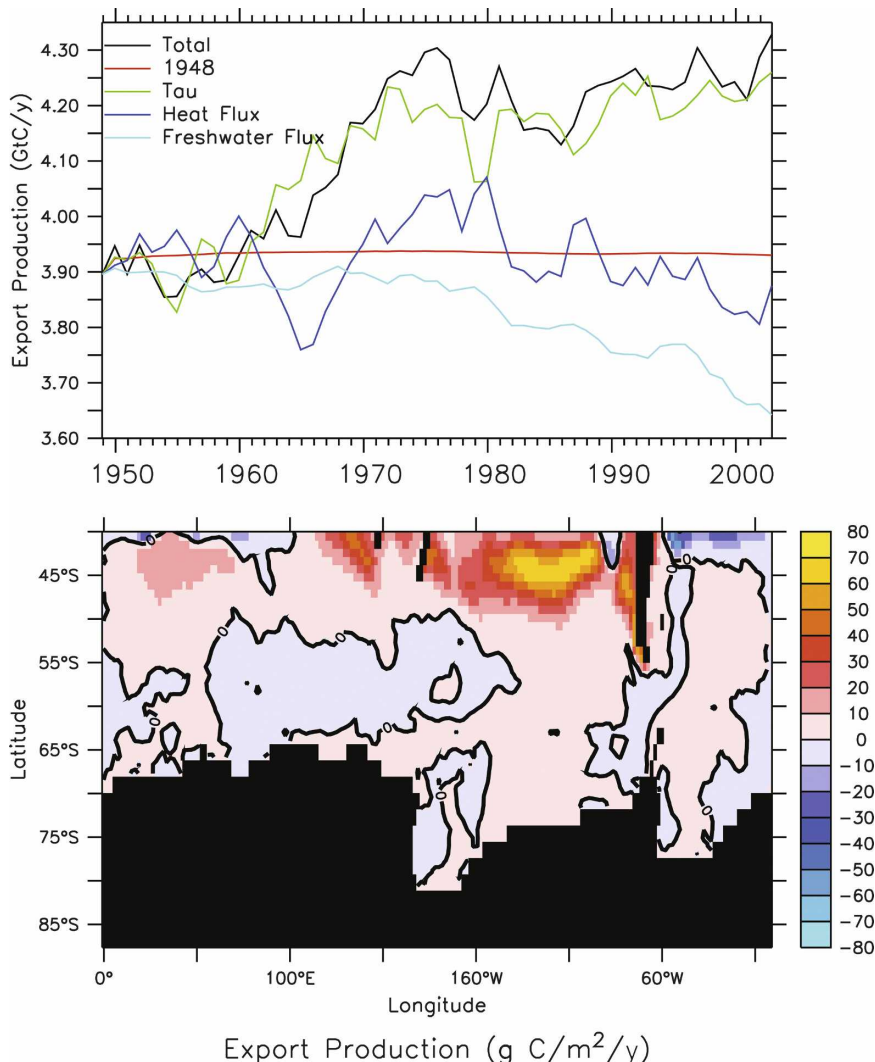


FIG. 6. Integrated SO annually averaged export production (Gt C yr^{-1}) for the various experiments following the color coding given in Fig. 4. For the year 2002, the difference in the annual averaged export production between the total experiment and 1948 experiment ($\text{g C m}^{-2} \text{ yr}^{-1}$).

temporally decoupled from the nutrient cycle. This allows for a reduction in the SO carbon uptake to occur, which will eventually be partially offset by increased carbon uptake when some of the elevated nitrate in the SAMW and AAIW is returned to the surface where it can stimulate more export production and cause the uptake of carbon from the atmosphere.

c. Sensitivity of carbon–climate response

To explore the simulated relationship in which the changes in the anthropogenic uptake are much smaller and opposite in sign to the changes in the natural carbon uptake, and to predict the future relationship between the natural and anthropogenic carbon uptake,

we used a simple box model representation of the SO (Fig. 7). In the SO box model, carbon-rich water is upwelled in the divergence region at a rate of q (s^{-1}), transported northward, and then subducted. In the surface box where this upwelling occurs we assumed that the carbon content of the box equilibrates with the atmosphere. The water is then subducted into the ocean interior. We used the box model to explore how changes in ocean ventilation (q) affect the anthropogenic and natural carbon uptake. Consistent with our BOGCM simulations we neglected the effect of changes in carbon export on the carbon uptake.

For the natural carbon cycle, the total carbon flux into the ocean was

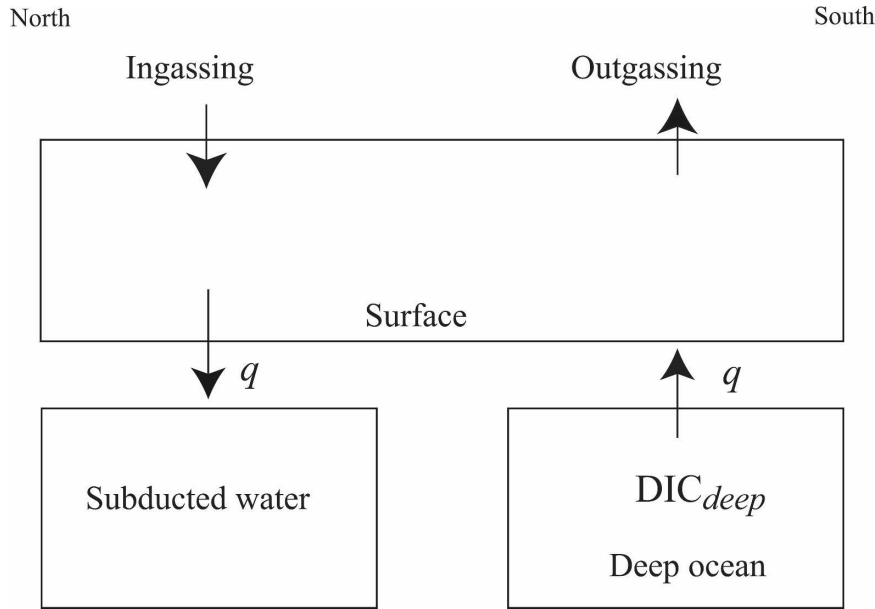


FIG. 7. Idealized box model of the SO representing the upwelling of carbon-rich deep water and its subsequent subduction.

$$F_N = q(\text{DIC}_{\text{PIA}} - \text{DIC}_{\text{deep}}), \quad (1)$$

where DIC_{deep} and DIC_{PIA} represented the DIC of the deep-ocean box and the DIC value of the surface in equilibrium with a preindustrial atmosphere, respectively. Changing the rate of ocean ventilation changed the natural carbon cycle flux by

$$\Delta F_N = \Delta q(\text{DIC}_{\text{PIA}} - \text{DIC}_{\text{deep}}). \quad (2)$$

Now, if the atmospheric CO_2 was increasing resulting from the emissions of anthropogenic CO_2 , the DIC of the surface box would also increase. Assuming that the increase in DIC of the surface box was $A(t)$, the total flux of carbon into the ocean is

$$F_T = q\{[\text{DIC}_{\text{PIA}} + A(t)] - \text{DIC}_{\text{deep}}\}, \quad (3)$$

where the anthropogenic flux and the change in the anthropogenic flux were given by

$$F_A = q[A(t)], \quad \Delta F_A = \Delta q[A(t)], \quad (4)$$

respectively. Therefore, the change in anthropogenic flux divided by the change in natural carbon flux was

$$\Delta F_A / \Delta F_N = -A(t) / (\text{DIC}_{\text{deep}} - \text{DIC}_{\text{PIA}}). \quad (5)$$

If we rewrite the equation in terms of pCO_2 we get

$$\Delta F_A / \Delta F_N = -[\text{pCO}_2^A(t) - 280] / (\text{pCO}_2^{\text{Deep}} - 280), \quad (6)$$

where $280 \mu\text{atm}$ was the preindustrial pCO_2 atmospheric value. For the period of the BOGCM simula-

tions, pCO_2^A varied between 310 and $370 \mu\text{atm}$. An estimate of the maximum deep-water pCO_2 value was approximately $430 \mu\text{atm}$ (McNeil and Matear 2007); in comparison the BOGCM simulations gave a value of about $450 \mu\text{atm}$. Using $450 \mu\text{atm}$ for the deep-ocean value gave a range from -0.17 to -0.55 for the ratio of the change in anthropogenic to natural carbon flux with an average value of -0.32 . For the past and for the next several decades the anthropogenic change in the oceanic uptake will be smaller and have the opposite sign to the change in the natural carbon uptake. The anthropogenic uptake change will only exceed the natural carbon change when the pCO_2 of the atmosphere is greater than the pCO_2 of the upwelled water. Our box model suggested that the anthropogenic response will dominate when atmospheric CO_2 exceeds $450 \mu\text{atm}$, which will occur in 2030 under emission scenario IS92A, which is consistent with future projections of SO carbon uptake (Zickfeld et al. 2007).

In developing the box model, there are three potential issues that may impact the ratio of changes in anthropogenic uptake to changes in natural carbon uptake given by Eq. (6). We now explore these three issues.

First, we assumed complete equilibration. In the SO, this may not occur because recently upwelled water may be subducted before being equilibrated with the atmosphere. The nonequilibrium of the subducted water would have a greater effect on the anthropogenic carbon uptake than the natural carbon uptake because

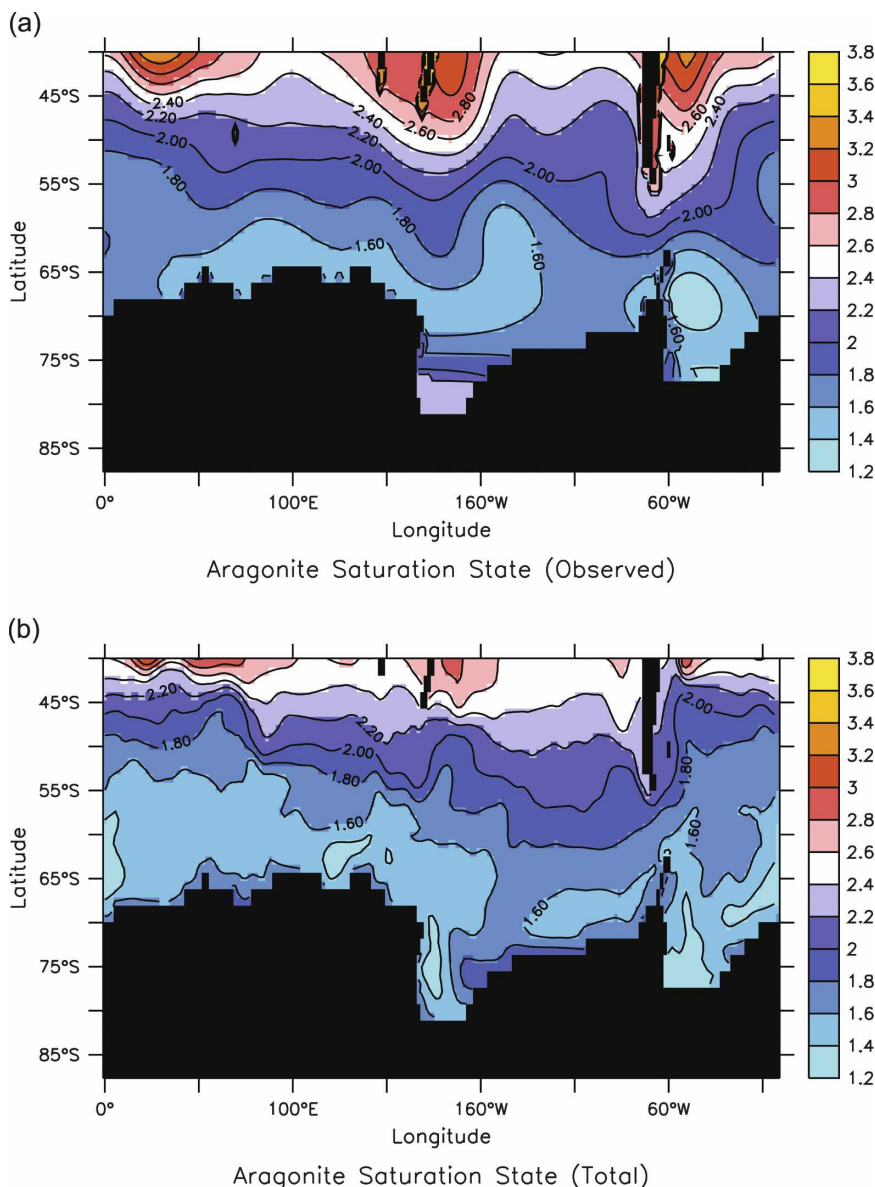


FIG. 8. For the year 1995, the aragonite saturation state calculated from the (a) observations and (b) 1948 experiment.

the peak in anthropogenic carbon uptake occurs north of where the peak in the natural carbon uptake occurs. Hence, the time the subducted water has to absorb the anthropogenic signal would be less than the time available to equilibrate the natural carbon cycle with the atmosphere. Therefore, we expect it would reduce the absolute value of the ratio.

Second, the surface ocean solubility of CO₂ may decline because of temperature, salinity, and alkalinity changes as simulated by the heat flux (Hflx) and freshwater flux (Fflx) experiments. This would be equivalent to increasing the deep-ocean pCO₂ value and this

would reduce the absolute value of the ratio of changes in anthropogenic uptake to changes in natural carbon uptake. In the BOGCM simulations, the solubility changes of the Hflx and Fflx experiments explain the reduction in ratio from -0.26 in the tau experiment to -0.12 and -0.22 in the Hflx and Fflx experiments, respectively. The solubility changes were greatest in the Hflx experiment, which produced the smallest absolute value of the ratio.

Third, the export of carbon from the upper ocean may change with ocean ventilation. However, as discussed in the previous section, increases in export pro-

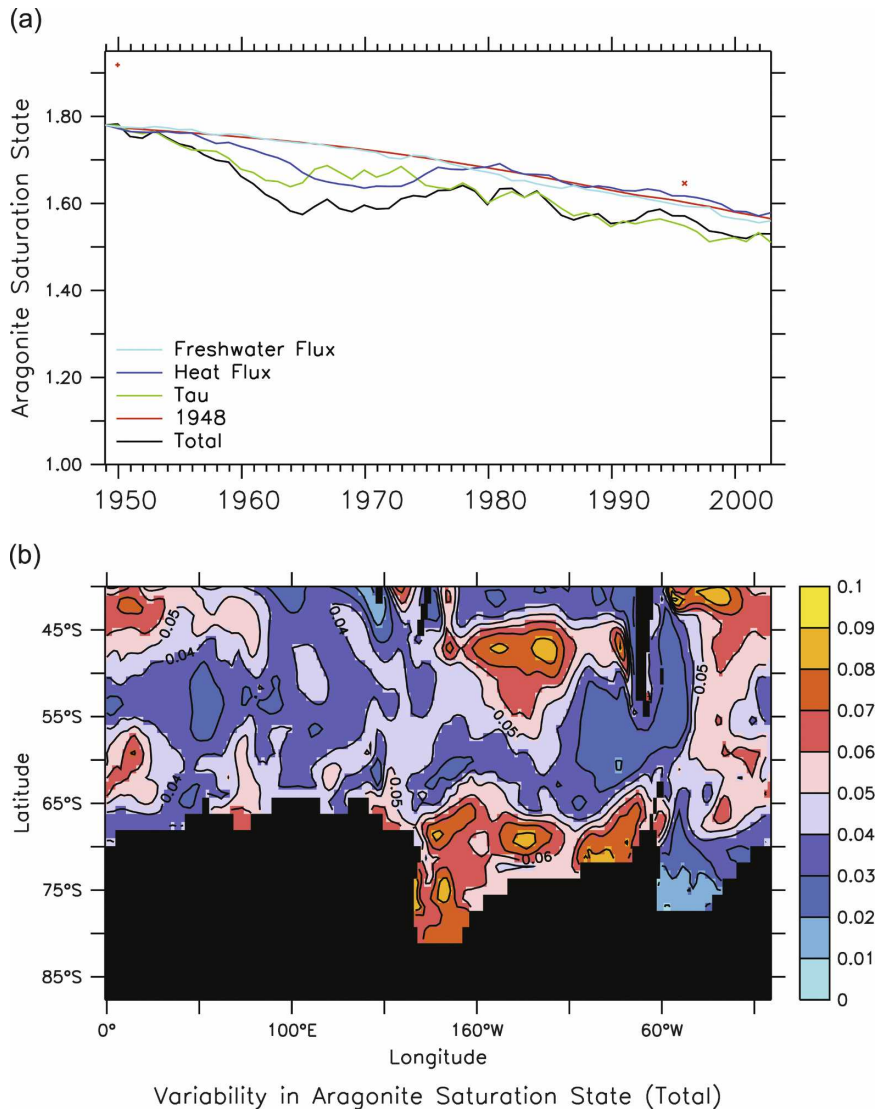


FIG. 9. (a) Annually averaged aragonite saturation state of the surface water south 60°S for the various experiments. The color coding of the lines is the same as Fig. 4. The two red points in the top panel denote the aragonite saturation state based on observations from 1995 and from preindustrial estimates of DIC. (b) In the total experiment, the one standard deviation variability in aragonite saturation state after the removal of decadal trend.

duction (EP) with increased ocean ventilation were expected to be small. An increase in EP with increased ocean ventilation would increase the natural carbon uptake by more effectively transporting the carbon to the deep ocean rather than to the atmosphere. This would cause the absolute value of the ratio to decrease.

These three caveats may slightly modify the relationship between changes in anthropogenic carbon uptake and changes in natural carbon uptake suggested by the box model. However, none of these caveats will alter the results that changes in the natural carbon uptake are greater than and opposite to the changes in

the anthropogenic carbon uptake for the historical period.

d. Aragonite saturation state

The increased ventilation of the SO did not only alter the air–sea fluxes of carbon, it also modified the water properties of the upper ocean and altered the carbon chemistry of the surface water. A key carbon parameter is the aragonite saturation state (Ω_A), which does influence the rate of calcification of marine organisms (Riebesell et al. 2000; Langdon and Atkinson 2005). The surface water of the SO has annual mean Ω_A that

generally is lowest in the divergence regions (south of 60°S) where the observed 1995 value is less than 1.6 (Fig. 8). The 1948 experiment showed a similar pattern to the observations but the values were generally about 0.1 less than the observations (Fig. 8). To gauge how the temporal evolution of Ω_A evolved under various atmospheric forcing experiments we plotted the annual mean surface Ω_A south of 60°S, where the values were most influenced by ocean ventilation. All forcing experiments showed a decline in Ω_A with time (Fig. 9). For comparison we also plotted the Ω_A based on the observed climatological SST and SSS (Conkright et al. 2002) and the present-day DIC and alkalinity (1995), and the estimated preindustrial DIC and alkalinity (Sabine et al. 2005). For the high-latitude SO, where the water had the lowest Ω_A values, the experiments with increased winds (total and tau) had the lowest aragonite saturation state. In the high-latitude region, DIC changes dominated the Ω_A differences between the various simulations (greater than 90% of the response). The increased DIC caused by increased ventilation of the SO reduces Ω_A in the surface ocean. The cooling of the SO in the 1960s produced a decline in Ω_A (blue and black lines in Fig. 9), and it was associated with increased ventilation of the high-latitude SO (Fig. 5b) and high DIC in the surface. Under a higher wind regime the transition to an SO that has a surface ocean that is undersaturated with respect to aragonite will occur sooner. The atmospheric forcing can also generate large interannual variability in Ω_A (Fig. 9b). The simulated interannual variability is highest in the Pacific sector of the SO. The large natural interannual variability may provide a means to investigate the impact of ocean acidification on SO marine ecosystems.

5. Conclusions

Historical climate change provides an ideal situation to investigate how the SO carbon uptake varies to provide insight into how global warming will influence the future carbon uptake (i.e., the strengthening of the SAM). The trend in the winds and the heat and freshwater fluxes over the 1948–2002 period produced complex and opposing responses on the SO carbon uptake and on the surface ocean Ω_A . The uncertainty in the SO atmospheric forcing data makes the SO uptake response to historical climate change sensitive to how the data are used to force the ocean model. The use of atmospheric data can lead to either our result of little change in the SO carbon uptake over the last three decades or to Le Quere et al.'s (2007) results of a decline in the SO uptake.

The results from our box model are consistent with

the BOGCM response that over the historical period the changes in the natural carbon uptake were greater and opposite to the changes in the anthropogenic carbon uptake. However, if the climate change trends continue, in the future with higher atmospheric CO₂ levels, the changes in the anthropogenic carbon uptake will eventually exceed the changes in the natural carbon uptake leading to increased carbon uptake by the SO. Improved observational effort to document how the SO responds to changes in atmospheric forcing is crucial to understanding how changes in atmospheric forcing will impact carbon uptake and cycling (IOCCP 2007). The development and implementation of an observing strategy to monitor interannual variability should be given high priority given the important role the SO plays in mitigating the rise in atmospheric CO₂ by absorbing our anthropogenic carbon emissions. Further, model projections suggest that SO will be driven to aragonite undersaturation by the end of this century (Orr et al. 2005) and they show how changes in the ability of marine organisms to calcify will affect the ecosystem is of great concern. The simulated variability in the SO surface Ω_A suggests that interannual variability could also be used to investigate how ocean biota respond to the Ω_A changes.

Acknowledgments. RJM would like to acknowledge the funding support from the Australian Climate Change Science Program and the CSIRO Wealth from Oceans Flagship. AL was financially supported by the European Integrated Project CARBOOCEAN 511176.

REFERENCES

- Arblaster, J. M., and G. A. Meehl, 2006: Contributions of external forcings to southern annular mode trends. *J. Climate*, **19**, 2896–2905.
- Aumont, O., C. Le Quere, and J. C. Orr, 2004: NOCES project: Interannual HOWTO. IPSL. [Available online at <http://www.ipsl.jussieu.fr/OCMIP/phase3/simulations/NOCES/HOWTO-NOCES.html#toc3>.]
- Bopp, L., P. Monfray, O. Aumont, J. L. Dufresne, H. Le Treut, G. Madec, L. Terray, and J. C. Orr, 2001: Potential impact of climate change on marine export production. *Global Biogeochem. Cycles*, **15**, 81–99.
- Buesseler, K. O., J. E. Andrew, S. M. Pike, and M. A. Charette, 2004: The effects of iron fertilization of carbon sequestration in the Southern Ocean. *Science*, **304**, 414–417.
- Cai, W., and T. Cowan, 2007: Trends in Southern Hemisphere circulation in IPCC AR4 models over 1950–99: Ozone depletion versus greenhouse forcing. *J. Climate*, **20**, 681–693.
- Chen, D., L. M. Rothstein, and A. J. Busalacchi, 1994: A hybrid vertical mixing scheme and its application to tropical ocean models. *J. Phys. Oceanogr.*, **24**, 2156–2179.
- Conkright, M. E., R. A. Locarnini, H. E. Garcia, T. D. O'Brien, T. P. Boyer, C. Stephens, and J. I. Antonov, 2002: *World Ocean Atlas 2001: Objective Analyses, Data Statistics and Fig-*

- ures, *CD-ROM Documentation*. NODC Internal Rep. 17, 17 pp.
- Enting, I. G., M. L. Wigley, and M. Heimann, 1994: Future emissions and concentrations of carbon dioxide: Key ocean/atmosphere/land analyses. CSIRO Division of Atmospheric Research Tech. Paper 31, 118 pp.
- Fyfe, J. C., and O. A. Saenko, 2006: Simulated changes in the extratropical Southern Hemisphere winds and currents. *Geophys. Res. Lett.*, **33**, L06701, doi:10.1029/2005GL025332.
- Gent, P. R., and J. C. McWilliams, 1990: Isopycnal mixing in ocean circulation models. *J. Phys. Oceanogr.*, **20**, 150–155.
- Hall, A., and M. Visbeck, 2002: Synchronous variability in the Southern Hemisphere atmosphere, sea ice, and ocean resulting from the annular modes. *J. Climate*, **15**, 3043–3057.
- IOCCP, 2007: Surface ocean CO₂ variability and vulnerabilities workshop. IOCCP Rep. 7, Paris, France, IOC/UNESCO, 100 pp.
- Kalnay, E., 1996: The NCEP/NCAR 40-Year Reanalysis Project. *Bull. Amer. Meteor. Soc.*, **77**, 437–471.
- Langdon, C., and M. J. Atkinson, 2005: Effect of elevated pCO₂ on photosynthesis and calcification of corals and interactions with seasonal change in temperature/irradiance and nutrient enrichment. *J. Geophys. Res.*, **110**, C09S07, doi:10.1029/2004JC002576.
- Law, R. M., R. J. Matear, and R. J. Francey, 2008: Comment on “Saturation of the Southern Ocean CO₂ sink due to recent climate change.” *Science*, **319**, 570.
- Lenton, A., and R. J. Matear, 2007: Role of the Southern Annular Mode (SAM) in Southern Ocean CO₂ uptake. *Global Biogeochem. Cycles*, **21**, GB2016, doi:10.1029/2006GB002714.
- , —, and B. Tilbrook, 2006: Design of an observational strategy for quantifying the Southern Ocean uptake of CO₂. *Global Biogeochem. Cycles*, **20**, GB4010, doi:10.1029/2005GB002620.
- Le Quere, C., and Coauthors, 2007: Saturation of the Southern Ocean CO₂ sink due to recent climate change. *Science*, **316**, 1735–1738, doi:10.1126/science.1136188.
- Löscher, B. M., H. J. W. De Barr, J. T. M. De Jong, C. Veth, and F. Dehairs, 1997: The distribution of Fe in the Antarctic Circumpolar Current. *Deep-Sea Res. II*, **44**, 143–187.
- Lovenduski, N. S., N. Gruber, S. C. Doney, and I. D. Lima, 2007: Enhanced CO₂ outgassing in the Southern Ocean from a positive phase of the Southern Annular Mode. *Global Biogeochem. Cycles*, **21**, GB2026, doi:10.1029/2006GB002900.
- , —, and —, 2008: Toward a mechanistic understanding of the decadal trends in the Southern Ocean carbon sink. *Global Biogeochem. Cycles*, **22**, GB3016, doi:10.1029/2007GB003139.
- Marshall, G. J., 2003: Trends in the Southern Annular Mode from observations and reanalyses. *J. Climate*, **16**, 4134–4143.
- Matear, R. J., and A. C. Hirst, 1999: Climate change feedback on the future oceanic CO₂ uptake. *Tellus*, **51B**, 722–733.
- , and —, 2003: Long term changes in dissolved oxygen concentrations in the ocean caused by protracted global warming. *Global Biogeochem. Cycles*, **17**, 1125, doi:10.1029/2002GB001997.
- McNeil, B. I., and R. J. Matear, 2007: Climate change feedback on future oceanic acidification. *Tellus*, **59B**, 191–198.
- , —, R. M. Key, J. L. Bullister, and J. L. Sarmiento, 2003: Anthropogenic CO₂ uptake by the ocean based on the global chlorofluorocarbon data set. *Science*, **299**, 235–239.
- Miller, R. L., G. A. Schmidt, and D. T. Shindell, 2006: Forced annular variations in the 20th century Intergovernmental Panel on Climate Change Fourth Assessment Report models. *J. Geophys. Res.*, **111**, D18101, doi:10.1029/2005JD006323.
- Orr, J. C., and Coauthors, 2005: Anthropogenic ocean acidification over the twenty-first century and its impact on calcifying organisms. *Nature*, **437**, 681–686.
- Pacanowski, R. C., and S. M. Griffies, 1999: The MOM 3 manual. NOAA/Geophysical Fluid Dynamic Laboratory Tech. Rep. 4, 580 pp.
- Reynolds, R. W., and T. M. Smith, 1994: Improved global sea surface temperature analyses using optimal interpolation. *J. Climate*, **7**, 929–948.
- Riebesell, U., I. Zondervan, B. Rost, P. D. Tortell, R. E. Zeebe, and F. M. M. Morel, 2000: Reduced calcification of marine plankton in response to increased atmospheric CO₂. *Nature*, **407**, 364–367.
- Rodgers, K. B., B. Blanke, G. Madec, O. Aumont, P. Ciais, and J.-C. Dutay, 2003: Extratropical sources of Equatorial Pacific upwelling in an OGCM. *Geophys. Res. Lett.*, **30**, 1084, doi:10.1029/2002GL016003.
- Russell, J. L., K. W. Dixon, A. Gnanadesikan, R. J. Stouffer, and J. R. Toggweiler, 2006a: The Southern Hemisphere westerlies in a warming world: Propping open the door to the deep ocean. *J. Climate*, **19**, 6382–6390.
- , R. J. Stouffer, and K. W. Dixon, 2006b: Intercomparison of the Southern Ocean circulations in IPCC coupled model control simulations. *J. Climate*, **19**, 4560–4575.
- Sabine, C. L., and Coauthors, 2005: Global Ocean data Analysis Project (GLODAP): Results and data. ORNL/CDIAC-145 NDP-083, 110 pp.
- Sarmiento, J. L., T. M. C. Hughes, R. J. Stouffer, and S. Manabe, 1998: Simulated response of the ocean carbon cycle to anthropogenic climate warming. *Nature*, **393**, 245–249.
- , N. Gruber, M. A. Brzezinski, and J. P. Dunne, 2004: High-latitude controls of thermocline nutrients and low latitude biological productivity. *Nature*, **427**, 56–60.
- Thompson, D. W. J., and S. Solomon, 2002: Interpretation of recent Southern Hemisphere climate change. *Science*, **296**, 895–899.
- Trull, T., S. R. Rintoul, M. Hadfield, and E. R. Abraham, 2001: Circulation and seasonal evolution of polar waters south of Australia: Implications for iron fertilization of the Southern Ocean. *Deep-Sea Res. II*, **48**, 2439–2466.
- Walsh, J., 1978: A data set on northern hemisphere sea ice extent, 1953–1976. Glaciological Data, World Data Center for Glaciology Report GD-2, 49–51.
- Wanninkhof, R., 1992: Relationship between wind speed and gas exchange over the ocean. *J. Geophys. Res.*, **97**, 7373–7382.
- Yin, J. H., 2005: A consistent poleward shift of the storm tracks in simulations of 21st century climate. *Geophys. Res. Lett.*, **32**, L18701, doi:10.1029/2005GL023684.
- Zickfeld, K., J. C. Fyfe, O. A. Saenko, M. Eby, and A. J. Weaver, 2007: Response of the global carbon cycle to human-induced changes in Southern Hemisphere winds. *Geophys. Res. Lett.*, **34**, L12712, doi:10.1029/2006GL028797.
- Zwally, H. J., C. Parkinson, W. Campbell, F. Carsey, and P. Gloerson, 1983: *Antarctic Sea Ice, 1973-1976: Satellite Passive Microwave Observations*. NASA, 206 pp.